Length-dependent force characteristics of coiled coils

Sara Sadeghi and Eldon Emberly
Physics Department, Simon Fraser University, Burnaby, British Columbia, Canada V5A 1S6
(Received 5 June 2009; published 14 December 2009)

Coiled-coil domains within and between proteins play important structural roles in biology. They consist of two or more α helices that form a superhelical structure due to packing of the hydrophobic residues that pattern each helix. A recent continuum model showed that the correspondence between the chirality of the pack to that of the underlying hydrophobic pattern comes about because of the internal deformation energy associated with each helix in forming the superhelix. We have developed a coarse-grained atomistic model for coiled coils that includes the competition between the hydrophobic energy that drives folding and the cost due to deforming each helix. The model exhibits a structural transition from a non-coiled-coil to coiled-coil state as the contribution from the deformation energy changes. Our model is able to reproduce naturally occurring coiled coils and essential features seen in unzipping experiments. We explore the force-extension properties of these model coiled coils as a function helix length and find that shorter coils unfold at lower force than longer ones with the required unfolding force eventually becoming length independent.

DOI: 10.1103/PhysRevE.80.061909 PACS number(s): 87.15.ak, 87.15.hm, 87.15.La

I. INTRODUCTION

Proteins are polymers whose three dimensional structure is built from simpler secondary structural elements: helical backbone sections called α helices or straight backbone sections called β strands. For a given protein, the final fold consists of a unique packing of its secondary structural elements. An examination of known protein structures reveals that the number of folds, consisting of a specific packing of secondary elements, is much smaller than the actual number of known protein structures [1]. One of the most ubiquitous folds is a coiled coil which consists of two or more α helices that wrap around each other to form a superhelical structure. They have several biological functions, from mediating protein-protein interactions to forming mechanically important structural elements, such as the necks of molecular motors (e.g., kinesin and myosin). Because they are often subject to mechanical stresses inside cells, understanding how they fold and respond to forces is of physical and biological interest.

For a given coiled coil, the superhelical structure and its stability are dictated by the underlying amino-acid sequence of the helices forming the coil. The superhelix forms due to the packing of repeating hydrophobic residues that wind around each alpha helix. Naturally occurring coiled-coils form left-handed superhelical structures caused by a repeating seven amino acid motif called a heptad repeat, which has hydrophobic residues placed at specific positions in the 7mer that generate a left-handed winding hydrophobic strip. However, by varying the sequence, other superhelical structures are possible (such as a right-handed coiled coil), and several have be rationally designed [2]. Thus coiled coils provide a model system for studying the relationship between protein sequence and structure.

The folding kinetics of coiled coils has been studied both in bulk using fluorescence techniques [3–5], and at the single-molecule level through the application of force to a single coiled-coil structure [6–9]. These studies have elucidated the folding trajectory of coiled coils and how stability depends on sequence. In particular, [6] provided a high-resolution map of the gradual unzipping of coiled coils of differing lengths. In this experiment, a single coiled-coil domain (leucine zipper) was subject to a loading force using an atomic force microscope (AFM) that pulled apart the coiled coil from one end, while the other end remained linked [see Fig. 1(a)]. They were able to see transitions corresponding to the sequential pulling apart of the superhelical turns. By fitting a multistate model to their data they were able to extract key folding parameters such as the energy to form a turn and nucleate the coiled coil, and how these depend upon the sequence of the underlying heptad repeat.

Recent theoretical work, using a continuum model for the α helices, has shown how the superhelical structure arises as a competition between the energy gained from packing the hydrophobic residues and the cost of deforming the helices [10]. In that work they showed that the structure which minimizes the total energy is a superhelix whose twist is the same as the underlying twist of the hydrophobic strip of each he

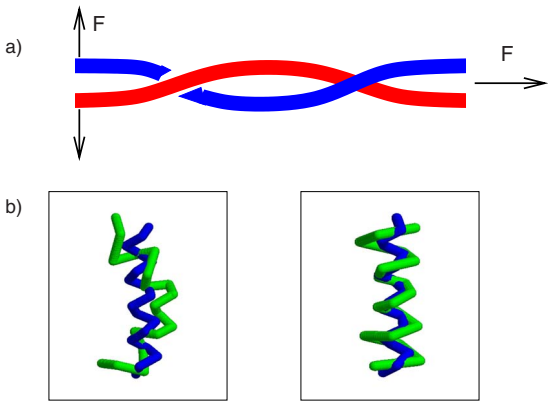

FIG. 1. (Color online) (a) Schematic of a coiled coil consisting of two α helices that wrap around each other to form a superhelical structure. We consider cases where the force is applied perpendicular or along the long axis of the coiled coil. (b) The deformations associated with the bend and twist normal modes of an α helix calculated from the spring model given in Eq. (3).

lix. In the absence of any energetic cost of deformation, they predict that it should be possible for a variety of different structures to form; all satisfying the criterion to pack the hydrophobic residues together.

To complement the above experimental and theoretical work, we have developed a coarse-grained atomistic model to study the formation of coiled coils and their mechanical properties under an applied load. Previous work explored the packing of rigid helices to study helix-bundle formation [11], and now we allow for the helices to have flexible degrees of freedom. To model coiled-coil formation we consider a simple energy function which consists of three contributions: a contribution from the hydrophobic energy gained by packing together the hydrophobic residues, an energetic cost for deforming each α helix, and finally the work done by applied forces to the coiled coil. In particular it is computationally efficient, using the collective motions (normal modes) of each helix [12] to explore the space of possible structures, analogous to the backbone parameterization used in [13]. For a range of parameters, this simple model is able to produce coiled coils as free-energy ground-state structures for sequences that have either left-handed or right-handed chirality. In the absence of any applied force, we examine how coiled-coil formation depends on the weight of the energetic cost to deform the helices. We find that there is a transition from a non-coiled-coil structure to a coiled-coil fold at a particular deformation cost. Also, simulated coiled coils fit well to naturally occurring ones over a broad parameter range. With a fixed set of parameters that can produce coiled-coil structures, we study the mechanical unfolding properties as a function of length. We apply a force perpendicular to the long axis of left-handed coiled coils to reproduce the unzipping results of single-molecule experimental work [6,8,9]. Our results are able to capture the essential features seen experimentally, including the effects of sequence mutation. We also consider applying a load parallel to the axis of right-handed coiled coils to see when the coiled coil will unwind as it is pulled along its length [see Fig. 1(b)]. For parallel load, we consider two possible experimental situations where both helices are being pulled or just one at a time. Most of the time we see a collective unfolding of the coiled coil where the unzipping or untwisting of the ends leads rapidly to the unwinding of the entire coil. In the case of parallel applied force for the right-handed coiled coils, we also find that the unfolding force is smaller for shorter coils that posses less than two superhelical turns in comparison to longer coiled-coil structures where it becomes roughly length independent. We find that the changes in the force required to unzip the coiled coils is not significant for different lengths. These predictions should be readily testable experimentally.

This paper is organized as follows: in Sec. II we present the details of our coarse grained model for the structure of coiled coils and the energy function used for folding, Sec. III presents the Monte Carlo (MC) approach that we use in simulating coiled-coil folding or unfolding, Sec. IV presents a comparison between left-handed coiled structures generated from our model and naturally occurring ones. Section V presents the results of unzipping the left-handed coiled coils, which has been done with two different approaches of constant speed and constant incremental force. Section VI presents results of using simulated annealing to find the free-energy ground-state structures of right-handed coils as a function of the deformation cost, and finally in Sec. VII we show the results of unfolding right-handed coiled coils of various lengths under a parallel applied load using our Monte Carlo approach.

II. ENERGY FUNCTION FOR COILED COILS

Coiled coils consist of two or more α helices that wrap around each other to form a superhelical structure. To represent the structure of each helix we use the C_α atoms of the helical backbone. Each undistorted α helix has 3.6 residues per turn, with a rise of 1.5 Å/residue and a helix radius, r_h=2.3 Å. The helices making up the coiled coil interact via the energy function that we now detail.

Instead of considering all of the different interactions that exist between the various amino acids, we assume that the residues are either hydrophobic (H) or polar (P) since the superhelical structure is driven to form primarily by the hydrophobic force. Besides the hydrophobic force, there is an energetic cost associated with deforming each helix. In our model, these are the two dominant energetic terms which govern coiled-coil formation. In addition to these two energies, we consider the application of applied forces that do work on the coiled coil. Putting these contributions together, we arrive at the total energy, E, of a coiled coil,

$$E = E_H + w_B E_B - \sum_i \vec{F}_i \cdot \vec{R}_i, \tag{1}$$

where E_H is the energy from hydrophobic contacts between the residues of helices in the structure, E_B is the associated energy due to deformations of the bonds of each helix, described by the spring model below, w_B is the associated weight of the bending energy to the overall energy, $\vec{F}_i$ is an externally applied force (e.g., an optical trap, and AFM), and $\vec{R}_i$ is the displacement between the first residues of both helices when an external force is applied perpendicular to the coiled-coil axis or the end-to-end displacement of the ith helix in the case of applying a parallel load.

To model the hydrophobic energy, E_H we use a Lennard-Jones 6–12 potential given by

$$E_H = \sum_{i \neq j}^{N_H} \sum_{k,l} \epsilon(t_k^i, t_l^j) \left[\left(\frac{r_0}{r_{k,l}^{i,j}} \right)^{12} - 2 \left(\frac{r_0}{r_{k,l}^{i,j}} \right)^{6} \right], \tag{2}$$

where the sum is over all pairs of residues between the N_H helices, with t_k^i being the type of the jth residue of the ith helix, and $r_{k,l}^{i,j}$ is the distance between the kth and lth residues of helices i and j. The energy of a given interaction is determined by $\epsilon(t_1, t_2)$, where $t=H$ or $t=P$, and where we take $\epsilon(H,H) > \epsilon(H,P) > \epsilon(P,P)$ with $\epsilon(H,H) > 2\epsilon(H,P)$ to favor separation of H and P.

The helices in a coiled coil are distorted from their ideal straight helical configuration and an energetic cost must be assigned to these distortions. We use a ball and spring model to represent the deformation energy of each helix. The parameters of the model (i.e., spring constants) were determined by fitting the resulting normal modes to the principal

deformations of alpha-helices in the protein data bank [12]. The model contains four springs: nearest neighbor, next- and next-next-nearest neighbors, and one for hydrogen bonding between the i and $i+4$ residues. The energy E_B is given by

$$E_B = \sum_i \sum_j \sum_{l=1}^{4} \frac{1}{2} k_l (\vec{r}^{\,i}_{j,j+l} - \vec{r}_l)^2, \tag{3}$$

where $\vec{r}^{\,i}_{j,j+l}$ is the vector between the j and $j+l$ residues of the ith helix. The parameters for the model are: $k_1=100$ Å^{-2}, $k_2=20$ Å^{-2}, $k_3=20$ Å^{-2}, and $k_4=7$ Å^{-2} and the spring rest lengths are $r_1=3.8$ Å, $r_2=5.4$ Å, $r_3=5.0$ Å, and $r_4=6.2$ Å.

In the next section we describe how we find the structure that minimizes the total energy, Eq. (1) using Metropolis Monte Carlo and a move set centered around the normal modes of each α helix.

III. GENERATING COILED-COIL STRUCTURES: USING NORMAL MODE MOVE SET

To study the formation and unfolding properties of coiled coils using the energy function outlined in Sec. II we use a MC simulation. Molecular dynamics has been applied to study the force response of coiled coils [14], but we have chosen to use MC, an approach that has been applied to study other unfolding and protein-protein interaction problems [15–19]. In any Monte Carlo simulation of protein structure, an appropriate move set must be chosen such that the space of possible structures can be fully sampled in a computationally reasonable amount of time [19]. Since moving each C_α atom individually would lead to inordinately long folding times, we have chosen to use the normal modes and the six translational and rotational degrees of freedom of each helix as a move set. We calculate the normal modes of an α helix using the spring model defined by Eq. (3) [12]. Each mode has a corresponding eigenvector, δx_i that gives the unit displacement from the undistorted helix [see, for example, the bend and twist modes in Fig. 1(b)]. Thus the coordinates of a deformed helix can be written as

$$\vec{x} = R(\phi,\theta,\psi) \cdot \left(\vec{x}_0 + \sum_i a_i \delta x_i \right) + \vec{T}, \tag{4}$$

where $\vec{x}$ contains the $3N$ coordinates of a N-residue helix, $\vec{x}_0$ are the coordinates of an undistorted helix, a_i is the amplitude of the ith normal mode, $R(\phi,\theta,\psi)$ is the rotation matrix corresponding to the rotation by the Euler angles, θ, ϕ, and ψ, and $\vec{T}$ is a translation of the helix in three-dimensional (3D). The $\{a_i\}$, $\{\theta,\phi,\psi\}$, and $\{T_i\}$ form the move set used in the Monte Carlo simulation, with corresponding step sizes δa_i. We adjust δa_i continually throughout the simulation to obtain a 50% acceptance rate for each move. Instead of using all the normal modes, only a fraction of the entire set are used—the low-energy collective motions of the residues making up the helix. Dependence on the results to this mode cutoff will be discussed below.

Starting from an unfolded state [see Fig. 2(a)], we obtain the lowest-energy structures of Eq. (1) using simulated annealing. The simulation starts with the N_h helices randomly oriented in space such that they do not intersect and that their centers of mass reside within a sphere of radius ≈ 10 Å. We use the following temperature schedule $T_{i+1}=T_i/\alpha$. We have found that using $1.75<T_0<2.5$ and $1.1<\alpha<1.2$ with eight or more temperature steps are able to constantly produce coiled-coil structures. We use on the order of 500 000 Monte Carlo steps at each temperature. For longer helices $L>70$ residues, we have also found that adding a random kick is useful at getting the simulation out of local minimum. The random kick is implemented by adding a kick probability p_{kick} and a kick amplitude, a_{kick}. At a given MC step, if a kick is successful, then a randomly selected mode's $\delta a_i = a_{kick}$. Using a $p_{kick}=0.1$ and $a_{kick}=10$ is adequate to get the longer coiled coils out of local energy minimal.

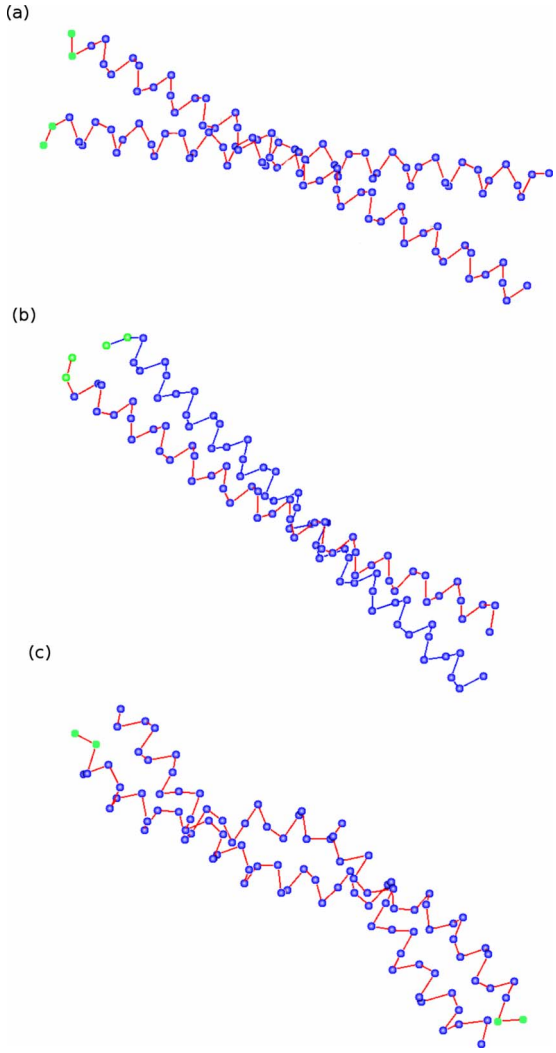

FIG. 2. (Color online) Structure of coiled coils formed from two 50mer α helices. (a) Initial random configuration of two undeformed α helices. (b) Final left-handed coiled-coil structure. (c) Final right-handed coiled-coil structure showing more than one full wind of the superhelix.

IV. GENERATING NATURALLY OCCURRING LEFT-HANDED COILED COILS

Most naturally occurring coiled coils are left handed, such as kinesin and myosin. Left-handed coiled coils form due to

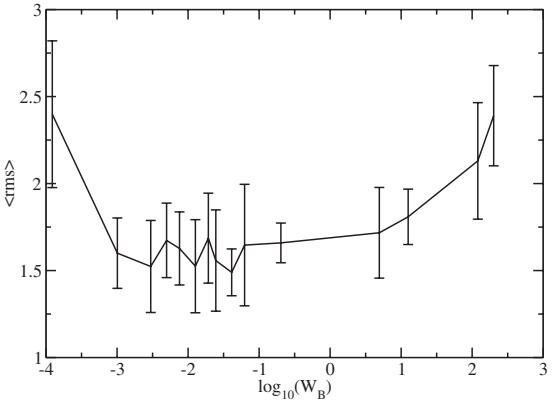

FIG. 3. Root-mean-square (rms) distance between simulated structures and crystal structure for GCN4 [20] as a function of deformation weight w_B. Shown is the average rms for ten structures generated at each value of w_B. Parameters for the model are given in the text.

a heptad repeat that has hyrophobic residues at the first and the forth positions. To study left-handed helices we have chosen the sequence repeat of the canonical leucine zipper GCN4 [20]. Structurally, each α-helical turn contain 3.5 residues and so each heptad contains two turns. In a leucine zipper the first and the forth positions of the heptad repeat are occupied by valine (V) and leucine (L) and every eight α-helical turns (28 residues), valine is replaced by asparagine (N) which is a polar amino acid. Given the leucine zipper sequence, we used our model to generate left-handed structures that could be compared to the naturally occurring one. The energies of interactions between residues were chosen to be $\epsilon(H,H)=3k_BT$, $\epsilon(H,P)=0.25k_BT$, and $\epsilon(P,P)=0.1k_BT$. [Making $\epsilon(H,P)$ as large as $1k_BT$ had little effect on the final coiled-coil structure]. We set the interaction distance between two residues to be $r_0=5.2$ Å. The parameters for the deformation energy are as in Sec. III, and it is scaled by w_B that has units of energy. An example of simulated coiled coils is shown in Fig. 2(b).

To get better insight into how the weight of deformation w_B changes the resulting coiled-coil structure, we calculated the root-mean-square (rms) distance between the simulated structures and the crystal structure for GCN4 from the protein data bank [20]. Specifically, for each value of w_B we generated ten structures and computed the average rms to the GCN4 structure (see Fig. 3). We found that using only 28 normal modes was sufficient to generate reproducible rms results. Higher modes had negligible amplitudes—this will cease to be the case when loads are applied to the coiled coils. As can be seen in Fig. 3 at low w_B, the cost of deformation is low resulting in structures with high pitch and hence a poor rms. At high w_B, the cost of deformation is so high that helices behave as rigid rods, resulting in a poor rms that plateaus above a certain w_B. However, there is a broad range of w_B where the rms is low (below 1.5 Å) showing that our simple energy model is capable of reproducing the shape of the naturally occurring leucine zipper.

V. UNZIPPING LEFT-HANDED COILED COILS

Recently, the mechanical properties of leucine zippers have been studied by unzipping them using single molecule approaches [6–9]. In particular, the force-extension curves of leucine zippers of different lengths as well as leucine zippers with point mutations have been measured [6]. These measurements revealed that the coil would unzip in stages under constant velocity pulling measurements and that point mutations where the asparagine (N) is substituted with valine (V) would lead to an overall stabilization of the coil [6]. Using our model, we simulated the experiments above by unzipping left-handed coils of differing lengths as well as coiled coils that possess point mutations.

In our simulation, we apply a load perpendicular to the axis of the coiled coil at the first residues of each helix in the coiled coil. We consider two different ways of applying the external force: one is by increasing the distance between the first residues of the helices using a constant displacement (i.e., AFM experiment) and the other is by using an incremental force. In both cases there is a spring between the third last residues of each helix acting as a cysteine bridge, preventing the end of the coil from separating, just as in experiments.

As in the experiment [6], we choose different lengths of leucine zipper with 10,18 and 26 α-helical turns referred to as LZ10, LZ18, and LZ26, respectively [21]. We used 24, 26, and 28 modes for each length, respectively. For the case of perpendicular pulling, adding more modes did not change the results of the unzipping simulations as the amplitudes of higher-order modes are negligible. We used $w_B=0.2$ and $T=1.0$ in all simulations.

For the constant displacement simulation, the separation between the first two residues is increased gradually by $\Delta\vec{d}$ and at each separation both helices equilibrate by MC. After equilibration we calculate the average energy of the structure and the average force from,

$$|\bar{F}_{i+1}| = \frac{\bar{E}_{i+1} - \bar{E}_i}{\Delta d}, \tag{5}$$

where $\bar{E}_i$ is the average energy at step i. The results presented below are for a choice of $\Delta d=1.0$ Å. Changing Δd is equivalent to pulling at different velocities, the results of which will be presented elsewhere. At each step the structure was relaxed for $\approx 2\times 10\,000 N_{mode}$ MC steps that works out to be $\approx$500 000 for the lengths of coils studied and we find that our unzipping results become insensitive to the number of MC steps used. A simulation stops when the coiled-coil fully unzips, marked by E_H going to near zero.

In Fig. 4, we show the calculated force-extension curves for the LZ10, LZ18, and LZ26 sequences. For each length, ten structures were generated and pulled ten times, and what is shown is the average force-extension curve from these runs. We first considered the situation of an "ideal" leucine zipper sequence where every N that occupies the first position of a heptad repeat is replaced by hydrophobic V [Fig. 4(a)]. As in the experiment, we see a staged unzipping, marked by rises and falls in the force as a function of length. Initially there is an increase in force required to break the hydrophobic contacts at the end, which then decreases as the coil becomes more unzipped. The number of stages increases with length, with the stages of the shorter coils occurring at

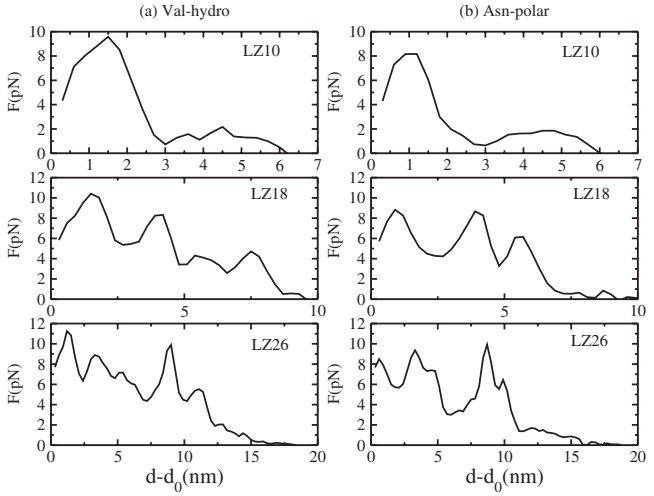

FIG. 4. Simulated force-extension curves for leucine zippers of differing lengths, LZ10, LZ18, and LZ26. (a) Results for sequences where Asn residues at the first position of heptad repeats replaced by Val. (b) Results for wild-type sequences that contain Asn residues at the first site of select heptad repeats.

the same locations in coils of longer length. LZ10 only displays a single transition, LZ18 has two clear stages, and LZ26 has three. For the longer helices, the sequence possess several runs of hydrophobic contacts that produce the transitions seen around 4 and 9 nm. We next consider the effects of changes in sequence. The wild-type sequences possess Asn residues in place of Val at certain heptads. We treat N as a *P*-type residue, though it is capable of forming hydrogen bonds which we neglect. Nevertheless, because of its polar character it is experimentally seen to have a destabilizing effect on the force-extension curves. As can be seen in Fig. 4(b) the substitution of Asn decreases the initial required force to unzip the first section of the coil, consistent with what was seen experimentally [6]. Its presence does not seem to change the number of stages in the unzipping process. Experimentally, only one N was changed to V in LZ18, so it will be interesting to see whether changing all the Ns to Vs has any effect on the number of unzipping stages.

We now move on to consider unzipping the coiled coils by applying a constant force perpendicular to the coil at the first residues of each helix. The force is gradually increased until the coil completely unzips [see Fig. 5(a)]. We define the transition force as the minimum force required to unzip the coiled coil. To locate this transition force we calculate the thermodynamic susceptibility of the hydrophobic energy defined as

$$\chi_H = \frac{dE_H}{dF}, \tag{6}$$

where E_H is hydrophobic energy and F is applied force. The transition force corresponds to the force where χ_H has its maximum value [see Fig. 5(b)]. There is only a single transition force, since once this force is met, the entire coil unzips since all the forces required to unzip the later stages are less than the first transition (see Fig. 4). For the results presented below, we used a force increment of

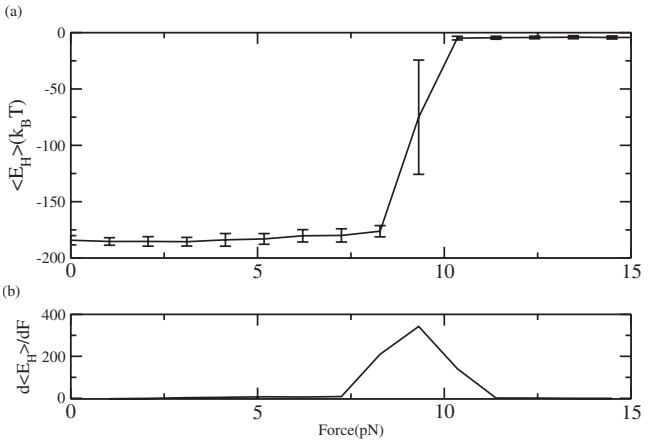

FIG. 5. (a) Average hydrophobic energy vs applied force for LZ18. (b) Thermodynamic susceptibility, Eq. (6) for the curve shown in (a). The unfolding or transition force is defined to be the force corresponding to the peak in the susceptibility.

$\Delta F = 0.25 k_B T/\text{Å}$. The pulling results depend on ΔF, with larger ΔF being equivalent to faster pulling rates, and these results will be presented elsewhere.

In Fig. 6 we show the calculated transition force as a function of leucine zipper length, from the smallest LZ10 to the longest LZ26. What is shown is the average transition force found from by pulling on ten different structures at each length, ten times. As can be seen the force needed to unzip coiled-coil structures that have Val substituted for Asn is higher, consistent with the observation that Val substitutions produce more stable structures [6]. The transition force is also seen to gradually increase with length for both wild-type and mutated sequences. This could have been inferred from the constant displacement results (Fig. 4) as the force of the first transition is seen to increase with length. This was also seen experimentally [6]. Hence our model confirms the experimentally observed increase in stability of longer leucine zippers.

We now move on to consider the mechanical properties of coiled coils under a parallel load and in particular right-handed coiled coils that form more superhelical turns per unit length.

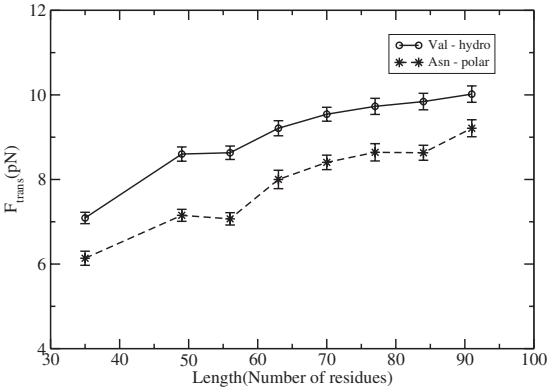

FIG. 6. Transition force for leucine zippers as a function of length. (Solid line) sequences with select Asn replaced with Val (see text). (Dashed Line) Wild-type leucine zipper sequences [21].

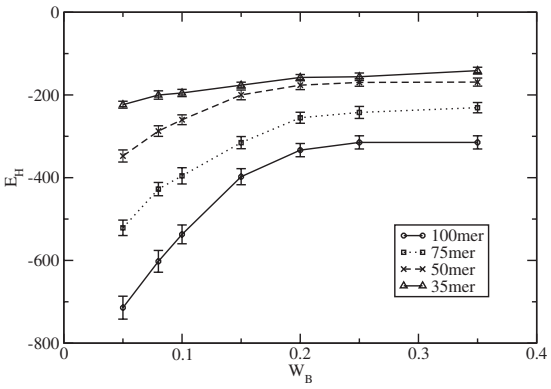

FIG. 7. Dependence of the average hydrophobic energy E_H on the weight of the deformation energy w_B for right-handed coiled coils patterned with HHPP sequence repeat. For a given w_B the average energy was computed using 15 different coiled-coil structures generated from the simulated annealing approach outlined in Sec. III.

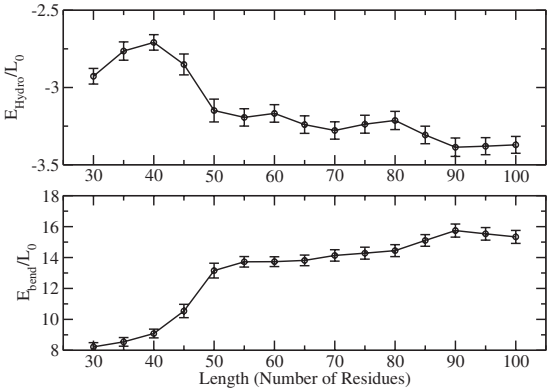

FIG. 8. Plot of (a) hydrophobic energy E_H and (b) deformation energy E_B as a function of length N. Each energy is normalized by N so that the y axis represents the energy or residue.

VI. DEPENDENCE OF RIGHT HANDED COILED-COIL STRUCTURE ON DEFORMATION ENERGY

As mentioned in Sec. IV most naturally occurring coiled coils are left handed although right-handed coiled coils have been rationally designed [2]. For coiled coils based on the heptad repeat sequence, the periodicities of the superhelical structures are on the order of 80–100 residues for the completion of one full wind. We have chosen to study helices patterned with a right-handed hydrophobic strip that has a periodicity of 32 residues so that several wrappings are possible for lengths $N<100$ residues. (Superhelical structures such as collagen although not built from α helices have multiple windings over a span of 100 residues). The sequence repeat that we chose to use which leads to a right-handed hydrophobic strip is a tetramer given by HHPP. We set the parameters as left-handed coiled-coil parameters and for the deformation energy are as in Sec. III.

Using the above parameters and the simulated annealing approach outlined in Sec. III, we generated sets of structures at different values of w_B. The resulting average energy of each set of structures is shown in Fig. 7. For $w_B>0.1$ the helices are essentially rigid rods and the resulting packs have higher energy. In this case the deformation energy E_B dominates and the stiff helices are not able to satisfy all their hydrophobic contacts. For long helices with 50 or more residues and at $w_B>0.2$, helices behave as rigid rods and the total energy no longer varies as w_B increases. For shorter helices, the energy does not plateau because due to their short length, they are able to make contacts between the hydrophobic residues at the both ends of helices. An example of a coiled-coil structure that is produced from the simulated annealing simulation is shown in Fig. 2(c). If w_B is made too small, then the hydrophobic residues cause unphysical compactification of the α helices. Hence in our simulations, we only ever see coiled-coil structures that adopt the same chirality as the hydrophobic strip that winds around each helix. In principle, if w_B was able to be made arbitrarily small, then it should be possible to see multiple structures emerge that satisfy the packing of the hydrophobic strip, as predicted in [10].

As mentioned in Sec. III, we do not use all the $3N$ normal modes of a helix of length N. In Fig. 9 we show the amplitudes of the normal modes in the final coiled-coil configuration at zero applied force, for the situation where 90 modes were used to make the structure. For modes above 30 the amplitudes are negligible and we find that we do not need to use them in generating the coiled-coil structures starting from an unfolded configuration. When the coiled coil is under an applied force, then this restriction is lifted as there are higher-order modes which do end up contributing to the unfolding process. This will be discussed in the following section.

To get further insight into how differences in the structure of coiled coils of different lengths affect the total energy, we compare the normalized bending and hydrophobic energy as a function of helix length (see Fig. 8) for coils generated using fixed $w_B=0.08$. For helices with $N<50$, the resulting coiled coils have less hydrophobic contact energy per residue than those which are longer. They also are less deformed from their ideal helical configuration and so have overall less deformation energy. Above $N=50$, the coiled coils form more than one complete superhelical wrapping and are able to satisfy more hydrophobic contacts. However, the better packing corresponds to larger deformations and hence an overall higher deformation energy than that of shorter helices. Nevertheless, at larger lengths the contact and deformation energy become length independent (see Fig. 8) showing that the resulting superhelical structure is periodic. Thus adding more residues just continues the established periodic structure.

VII. MECHANICAL UNFOLDING PROPERTIES OF RIGHT-HANDED COILED COILS

In many biological situations, such as for molecular motors whose necks consist of a coiled coil, the load is often exerted parallel to the axis of the coiled coil. In this section we consider the unfolding properties of the coiled-coil structures generated in Sec. VI subject to a force applied parallel

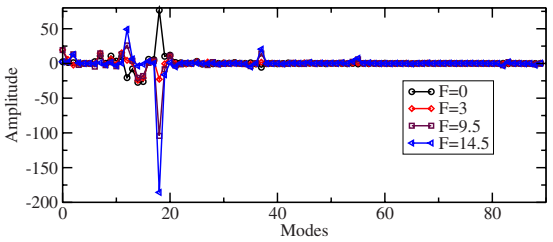

FIG. 9. (Color online) Amplitude of normal modes at different applied force for right-handed coiled coil with $N=100$. For this plot, both helices were being pulled simultaneously.

to their long axis (see Fig. 1 for a schematic). We consider the possibility of applying a force to just one or both of the helices. We use the Monte Carlo approach of unzipping the coiled-coil structures as described in Sec. V, except now the force is applied parallel to the coiled coil.

Under tension, the helices try to keep their hydrophobic contacts, but when the force is large enough their hydrophobic contacts break. As we discussed in Sec. V this force is called transition force. For most of the unfolding studies, just as for leucine zippers, we tend to see one large transition where the entire coiled-coil unfolds; there are smaller transitions, especially at initially low applied forces ($F<5k_BT/\text{Å}$) when the ends of the coiled coil fray slightly. The force corresponding to the peak in the thermodynamic susceptibility [Eq. (6)] we define as the transition force, F_{trans}. The transition force varies with length, and we now show how it changes depending on whether only one helix or both are pulled.

Before moving on to discuss the results of the pulling studies, we again comment on the number of normal modes used in carrying out the Monte Carlo simulation. When generating the coiled-coil structures in Sec. VI, we found that only ≈ 30 modes were necessary. Now when there is an applied load, we find that significantly more modes need to be included in order to generate consistent results. This is because there are higher-energy stretch modes which contribute to the unfolding process. This is shown in Fig. 9, where we show the mode amplitudes at different applied force. Some of the modes decrease in amplitude due to the unwinding of the coil (e.g., several of the modes between 10 and 20), whereas a number them increase (e.g., mode 19, 36, and 55) due to the stretching of the coil. We have found that using more than 30% of the modes for a given length produces consistent transition forces (see Fig. 10). Using lesser modes causes the transition force to be higher across all lengths and there was far more variation as a function of length.

We now discuss the results for the case of pulling on just one of the helices. For small coiled coils with 45 or less residues. there is no transition force—the coiled coil smoothly unwinds. For longer lengths the helix on which no force is applied stretches along with the other, and then at the transition force, it springs free, returning to its relaxed undeformed configuration. In Fig. 11(a), we plot the transition force as a function of length. For coiled coils above $N=60$, the structure consists of two or more full windings, and we see an increase in the force needed to unfold the coiled coil. There is some variation in the force as a function of length,

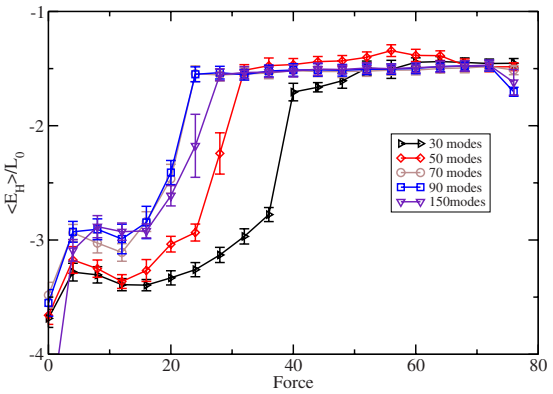

FIG. 10. (Color online) Dependence of unfolding as a function of the number of modes. Shown is the average hydrophobic energy per unit length as a function of force for $N=90$ using different normal mode cutoffs.

and we attribute this to the shearing that happens for some structures since residues on the ends that are being pulled do not line up perfectly along the long axis of the coil. Thus there will be periodic changes with length as the end-to-end vector departs from being parallel to the long axis.

For the case when both helices are being pulled, we applied an equal force to both. Thus the total load is twice that of case when one helix was being pulled. Because both helices are being pulled, they tend to stretch in unison, thereby being able to maintain their hydrophobic contacts. Now for all studied lengths, $N\geq 30$, we find that there is a transition force where the coil unfolds. The transition force as a function of length for the case where both helices are pulled is shown in Fig. 11(b). Similar to that found for the case where only one of the helices was pulled, we find that smaller coils unfold at lower forces than longer coils ($N>60$). It also takes about twice the force of that applied to a single helix to unfold the coil. For lengths greater than 60 residues, the force required to unfold the coil is essentially length independent. Some variation with length is again observed, and

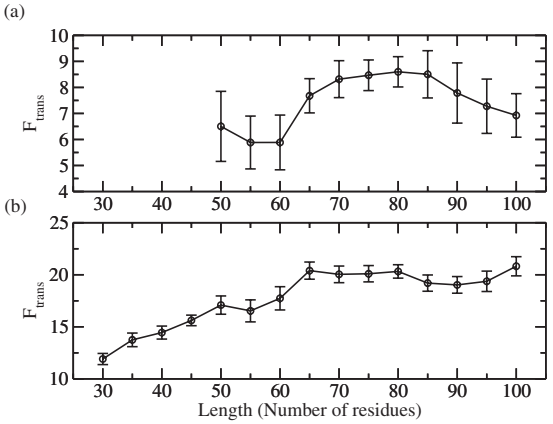

FIG. 11. Transition force, corresponding to the force at which the coiled coil loses most or all of its superhelical structure, as a function of right-handed coiled-coil length for pulling on (a) one helix or (b) both helices.

as before we attribute this to the change in the amount of shear that occurs as the length of the coil changes.

VIII. DISCUSSION

In summary, we have presented a simple energy model for coiled-coil formation and a computational approach that allows for the efficient generation of coiled-coil structures. Because of its simplicity and dependence on relatively few parameters, it can be adjusted to accommodate a variety of different coiled-coil structures.

We first used the model to study the folding properties of leucine zippers. Using just two types of residues, hydrophobic, and polar, the model was able to fit the naturally occurring leucine zipper GCN4. We then simulated the unzipping of leucine zippers of differing lengths and with point mutations. Our model was able to capture all of the essential results seen experimentally [6] such as staged unfolding when pulled at constant velocity, increased stability of coils when Val is substituted for Asn, and the overall increase in stability with coiled-coil length. The effects of pulling at different velocities can easily be incorporated into the model and this will be a subject of future research.

With respect to the prediction that it is the deformation energy that selects for the chirality of the resulting coiled-coil structure [10], our work has made some progress at addressing this prediction using an atomistic model. At a particular cost for the deformation energy, the model transitions from generating noncoiled structures as the α helices are too rigid, to coiled coil structures, where the superhelical twist matches that of the underlying hydrophobic strip that patterns each helix. However, when the deformation energy was given a small weight, we were unable to generate structures whose twist departed from that of the hydrophobic strip with the resulting structures possessing unphysical distortions. Future work will focus on keeping weight on the high-energy deformations, thus preserving the structural integrity of the α helices while allowing the energetic cost associated with the collective motions to be made arbitrarily small. This should allow us to explore the possibility of generating coiled-coil structures with chiralities that are different from that of the hydrophobic strip when there is little or no deformation cost.

Our results from studying the mechanical unfolding properties of right-handed coiled coils suggest several interesting predictions. First, when pulled along the long axis, we consistently find that in nearly all unfolding simulations, the coiled coils unfold in one large transition. We also found that coils that possess less than two full superhelical wrappings unfold at lower force than those that possess more. Additionally, pulling on both helices simultaneously will require a higher force to unfold the coil than the situation when only one helix is pulled. Current experiments have applied forces perpendicular to the long axis of the coil, but we expect that it should be relatively straightforward to pull along the long axis as has been done for other coiled-coil structures such as fibrin [22]. Thus these predictions should be readily tested. It will be interesting to see whether the coil unwinds before the hydrogen bonds that form the secondary structure of the α helices break as these energies are of similar magnitude. In our model we have separated these effects considering only the unwinding due to the breaking of the hydrophobic contacts. Adjusting the spring model to allow for the breaking of bonds is a topic for future work.

Because of the chiral nature of coiled-coil structure, using experimental approaches such as magnetic tweezers that allow for the application of torque will be of interest. Magnetic tweezers have been used to apply torque to study the winding of DNA [23,24], and they could be applied to coiled coils to study both the uncoiling and supercoiling of the superhelical structure. Incorporating torque is relatively straightforward in our model and will be explored in future work.

Lastly, naturally occurring coiled coils possess sequence disorder, namely, there are positions along the sequence that differ from the repeating heptad unit. Prior work has made progress on identifying how substitutions affect the stability of the resulting fold in specific situations. Using our model it should be possible to quantify how the distribution of disorder affects the stability and kinetics of coiled-coil formation. Preliminary results suggest that strategically placed sequence disorder can drastically speed up the kinetics of folding, allowing the coiled coil to escape otherwise low-lying energetic traps. It will be interesting to see if naturally occurring coiled coils exploit sequence disorder to alter the kinetics, besides just affecting stability.

ACKNOWLEDGMENTS

S.S. and E.E. would like to thank Nancy Forde and Dave Boal for helpful comments. E.E. would like to acknowledge the support of NSERC and the Canadian Institute For Advanced Research in carrying out this research.

[1] A. G. Murzin, S. E. Brenner, and T. Hubbard, and C. Chothia, J. Mol. Biol. **247**, 536 (1995).
[2] P. B. Harbury, J. J. Plecs, B. Tidor, T. Albert, and P. S. Kim, Science **282**, 1462 (1998).
[3] H. Wendt, C. Berger, A. Baici, R. M. Thomas, and H. R. Bosshard, Biochemistry **34**, 4097 (1995).
[4] L. B. Moran, J. P. Schneider, A. Kentsis, G. A. Reddy, and T. R. Sosnick, Proc. Natl. Acad. Sci. U.S.A. **96**, 10699 (1999).
[5] D. S. Talaga, W. L. Lau, H. Roder, J. Tang, Y. Jia, W. F. DeGrado, and R. M. Hochstrasser, Proc. Natl. Acad. Sci. U.S.A. **97**, 13021 (2000).
[6] T. Bornschlögl and M. Rief, Phys. Rev. Lett. **96**, 118102 (2006).
[7] I. Schwaiger, C. Stattler, D. R. Hostetter, and M. Rief, Nature Mater. **1**, 232 (2002).
[8] T. Bornschlögl and M. Rief, Langmuir **24**, 1338 (2008).
[9] T. Bornschlögl, G. Woehlke, and M. Rief, Proc. Natl. Acad. Sci. U.S.A. **106**, 6992 (2009)..

[10] S. Neukirch, A. Goriely, and A. C. Hausrath, Phys. Rev. Lett. **100**, 038105 (2008).
[11] E. G. Emberly, N. S. Wingreen, and C. Tang, Proc. Natl. Acad. Sci. U.S.A. **99**, 11163 (2002).
[12] E. G. Emberly, R. Mukhopadhyay, N. S. Wingreen, and C. Tang, J. Mol. Biol. **327**, 229 (2003).
[13] P. B. Harbury, B. Tidor, and P. S. Kim, Proc. Natl. Acad. Sci. U.S.A. **92**, 8408 (1995).
[14] R. L. C. Akkermans, and P. B. Warren, Philos. Trans. R. Soc. London, Ser. A **362**, 1783 (2004).
[15] V. Nanda and W. F. DeGrado, J. Am. Ceram. Soc. **128**, 809 (2006).
[16] H. Abe and H. Wako, Phys. Rev. E **74**, 011913 (2006).
[17] K. Eom, D. E. Makarov, and G. J. Rodin, Phys. Rev. E **71**, 021904 (2005).
[18] A. Kleiner and E. Shakhnovich, Biophys. J. **92**, 2054 (2007).
[19] J. Shimada, E. L. Kussell, and E. I. Shakhnovich, J. Mol. Biol. **308**, 79 (2001).
[20] E. K. O'Shea, J. D. Klemm, P. S. Kim, and T. Alber, Science **254**, 539 (1991). The PDB ID for GCN4 is 2ZTA. The sequence of GCN4 is MKQLEDK VEELLSK NYHLENE VARLKKL VGER. Our HP translation is PPPHPPPHPPHHP-PPHPHPPPHHPHPPHHPPP.
[21] The leucine-zipper sequences reproduced from [6] are **LZ10** MKQLEQK VEELLQK **N**YHLEQE VARLKQL VGECEGL, **LZ18** MKQLEQK VEELLQK **N**YHLEQE VARLKQL VGELEQK VEELLQK **N**YHLEQE VGECEGL, **LZ26** MKQLEQK VEELLQK **N**YHLEQE VARLKQL VGELEQK VEELLQK **N**YHLEQE VARLKQL VGELEQK VEELLQK **N**YHLEQE VARLKQL VGECEGL. The Asn highlighted in bold are locations where we substitute in Val. Our HP translations are: **LZ10** PPPHPPP HPPHHPP PHPHPPP HHPHPPH HPPHPPH, **LZ18** PPPHPPP HPPHHPP PHPHPPP HHPH-PPH HPPHPPP HPPHHPP PHPHPPP HPPHPPH, **LZ26** PP-PHPPP HPPHHPP PHPHPPP HHPHPPH HPPHPPP HPPH-HPP PHPHPPP HHPHPPH HPPHPPP HPPHHPP PHPHPPP HHPHPPH HPPHPPH.
[22] W. Liu, L. M. Jawerth, E. A. Sparks, M. R. Falvo, R. R. Hantgan, R. Superfine, S. T. Lord, and M. Guthold, Science **313**, 634 (2006); A. E. X. Brown, R. I. Litvinov, D. E. Discher, P. K. Purohit, and J. W. Weisel *ibid.* **325**, 741 (2009).
[23] A. Celedon, I. M. Nodelman, B. Wildt, R. Dewan, P. Searson, D. Wirtz, G. D. Bowman, and S. X. Sun, Nano Lett. **9**, 1720 (2009).
[24] R. Fulconis, A. Bancaud, J. F. Alleman, V. Croquette, M. Dutreix, and J. L. Viovy, Biophys. J. **87**, 2552 (2004).